Desalination and Water Treatment
www.deswater.com
doi: 10.5004/dwt.2020.25992

201 (2020) 31–42
October

Electro-hydraulic proportional control based pressurization and energy recovery integrated system in seawater desalination system

Wenlei Li[a], Jingyi Zhao[a,*], Guogang Wang[b], Qisheng Zhang[a], Kaixuan Jin[a], Qian Zhang[c], Lin Yu[b], Rui Guo[a]

[a]*School of Mechanical Engineering, Yanshan University, Qinhuangdao 066004, China, emails: zjy@ysu.edu.cn (J. Zhao), 1309116270@qq.com (W. Li), 13933953612@ysu.edu.cn (Q. Zhang), 1442933966@qq.com (K. Jin), guorui@ysu.edu.cn (R. Guo)*
[b]*Yongchunjie Seawater Desalination Technology Engineering Co., Ltd., Qinhuangdao 066004, China, emails: 13315668515@163.com (G. Wang), 13313333317@163.com (L. Yu)*
[c]*The Institute of Seawater Desalination and Multipurpose Utilization, MNR (Tianjin) 300110, China, email: sdzpzq@126.com (Q. Zhang)*

Received 6 September 2019; Accepted 8 April 2020

ABSTRACT

Seawater reverse osmosis (SWRO) has become an important method to solve the water shortage. In order to reduce energy consumption, the energy recovery device is widely used in the SWRO system. In this paper, an electro-hydraulic system is proposed to simultaneously realize raw seawater pressurization and energy recovery. The hydraulic cylinder and seawater cylinder are rigidly connected, and the pressurization and output flow of raw seawater is controlled by coordinating the motion state of the two hydraulic cylinders. The mathematical model of the system was established, and the feasibility and performance of the electro-hydraulic proportional control based pressurization and energy recovery system were verified by means of simulation and experiment. The results show that the pressure and flow fluctuation of raw seawater is small, and the energy consumption of produced water reaches 2.76 kWh/m^3, which is lower than that of conventional seawater desalination equipment.

Keywords: Seawater desalination; Energy recovery integrated device; Electro-hydraulic proportional control

1. Introduction

Water resources crisis has become one of the major challenges mankind is facing in the 21st century [1,2], which restricts economic and social development, seriously affects people's quality of life, and poses a serious threat to human health [3,4]. Seawater desalination has become the most effective means to solve the water resources crisis [5]. At present, the main methods of seawater desalination are reverse osmosis (RO), multi-stage flash evaporation, low-temperature multi-effect method, vapor compressing, etc. [6,7]. Seawater reverse osmosis (SWRO) is the most widely used method, by virtue of high efficiency and low cost [8,9]. However, the cost of producing freshwater using the RO technology remains high as much as 1.25 to 2.5 times, compared to supplying directly from a freshwater source [10]. In the SWRO system, the electricity charge accounts for about half of the cost for producing water, making reducing power consumption particularly important [11]. The main ways to reduce power consumption are to apply energy recovery devices (ERD), reduce the power of high-pressure pumps, and adopt new RO membrane technology or equipment. ERD can reduce specific energy consumption (SEC) by recovering pressure energy in waste concentrated seawater, and becomes an important part of (SWRO) systems [12].

* Corresponding author.

At present, there are two types of ERD on the market centrifugal type ERD and positive displacement type ERD. The latter directly converts pressure energy. With no intermediate link, the efficiency is over 90%. Therefore, positive displacement type has become the most efficient ERDs in the market place and has been globally adopted into SWRO systems [13].

The piston ERD are mainly driven by hydraulic pressure and electric drive, Song et al. [14,15] proposed a water hydraulic actuator driven by the high pressure (HP) brine of the desalting system. Long-term demonstration in the nanofiltration desalination system proves that the reciprocating-switcher energy recovery device (RS-ERD) with a water hydraulic actuator has good operational reliability whose pressure pulsation has been dramatically minimized to 3.3% while maintaining the efficiency as high as 96%. And in order to ensure system security, control logic and strategy for the emergency condition of the piston type energy recovery device is proposed. RS-ERD usually causes a significant fluid fluctuation of the device during stroke switching. To solve the problem, a modified RS-ERD with pilot valve plates was designed. The pressure fluctuation amplitude in HP fluids was declined by 40% under the pressure of 6.00 MPa [16]. Liu et al. [17,18] carried out numerical modeling simulation researches on the ERD of the new isobaric full rotary valve and proposed an optimized bilateral seal structure. Compared with a fully-rotary valve energy recovery device (FRV-ERD) with the original seal, the efficiency of FRV-ERD with the optimized bilateral seal is improved from 89.48% to 96.33%. Double work exchanger energy recovery and SalTec DT are two typical commercial products of the isobaric ERDs [19,20]. Schafer [21] designed a single-cylinder energy recovery devices (SC-ERDs), which solved the problem of high installation accuracy of double cylinder ERD. Wang et al. [22] put forward a new type of single-piston ERD, their experimental results show that two SC-ERDs in parallel have reached the basic function of the double-cylinders energy recovery devices (DC-ERD). The pressure fluctuation of the SC-ERD has been reduced about 80% compared with the DC-ERD under the same operating conditions and the energy recovery efficiency could still be remained as high as 98%. There are few theoretical design methods and simulation studies on ERD in a small RO desalination system. Sun et al. [23] proposed a mechanical-hydraulic ERD and mathematical model design method suitable for small-scale seawater desalination systems. The influence of piston and piston-rod area ratio and water recovery ratio on energy consumption was studied. The simulated results show that the hydraulic energy recovery device plays an important role in decreasing the SEC of the SWRO system from 10 to 3.0 kWh/m^3.

On the other hand, in recent years, research has begun on new technologies and equipment with high efficiency and energy-saving features based on the principle of RO. According to previous studies, the SEC of the RO desalination unit with ERD is about 2.4–3.8 kWh/m^3 [24,25]. Chong et al. [26] introduced the novel energy-efficient reverse osmosis (EERO) process that combines single-stage reverse osmosis (SSRO) with either a 2-stage or a 3-stage counter-current membrane cascade with recycle to increase the water recovery while reducing osmotic pressure differential (OPD) [26]. Kim et al. [27] presented split partial single-pass reverse osmosis (SSP RO) for the first time and investigated its performance using computer modeling. SSP RO is a design in which the permeate from the rear RO element(s) in a pressure vessel is blended with the RO feed, SSP RO produced an approximately 15% purer permeate compared to conventional single-pass RO [27]. Göktuğ Ahunbay [10] proposed a low-pressure high-recovery (LPHR) multistage RO desalination process that has 4-stage and 5-stage configurations. The performance of LPHR was evaluated under different conditions. The results show that the SEC of 4-stage configurations is 2.598 kWh/m^{3}and that of 5-stage configurations is 3.432 kWh/m^3 under 65% water recovery. Chong et al. [28] studied the performance of the EERO process considering the efficiency of pumps and ERD, The results show that the 3-stage EERO process has a lower SEC when an ERD is used (SECnet) compared to conventional SSRO for all overall water recoveries above 58.5%. The 4-stage EERO process has a lower SECnet compared to conventional SSRO, with overall water recoveries above 75.0%. Jeong et al. [29] established a high-efficiency RO membrane process model and optimized the EERO process. Under the conditions optimized, EERO exhibited greater energy efficiency (3%–25%).

The above ERD and energy-saving methods have achieved some results, but booster pumps and high-pressure pumps as well as special driving devices are needed. In this paper, an electro-hydraulic proportional control based pressure and energy recovery integrated system and corresponding control strategies are proposed, and a new system mathematical model and simulation platform is established. The feasibility of the innovation system and method is determined by mutual verification, and parameters relating to the system performance are analyzed.

2. Tools and methods

2.1. Energy recovery and pressure integrated device

In the integrated system of electro-hydraulic proportional control based pressurization and energy recovery, the traditional RO membrane method is applied to obtain potable freshwater.

In order to improve the efficiency and performance of the ERD, a controllable energy recovery seawater cylinder is invented, as is shown in Fig. 1. The volume of seawater cylinder with a rod chamber is filled with concentrated seawater, the volume of the rodless chamber of seawater cylinder is filled with raw seawater. The ratio of the area of the piston rod without rod end to the area of the ring with rod end is the ratio of the flow of the raw seawater and the concentrated seawater. Therefore, the ratio of rod end area to the rod end ring area can be changed to adapt to the different water recovery rate of RO desalination system. When the piston moves to the right, the low pressure (LP) raw seawater enters into the rodless end of the seawater cylinder through the LP raw seawater inlet valve 9, at this time, due to the spring force and LP of the HP raw seawater discharge valve 10, the HP raw seawater discharge valve 10 is closed, therefore, the raw seawater will not flow out through the HP raw seawater discharge valve 10. At the same time, the

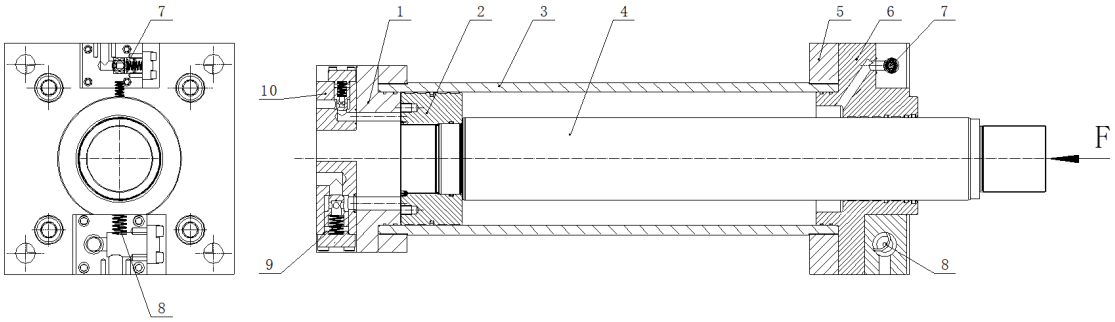

Fig. 1. Energy recovery and pressure integrated device. (1) End cover of seawater cylinder; (2) piston; (3) cylinder block; (4) piston rod; (5) front cover of seawater cylinder; (6) concentrated seawater integrated valve block; (7) HP concentrated seawater inlet valve; (8) LP concentrated seawater discharge valve; (9) LP raw seawater inlet valve; (10) HP raw seawater discharge valve.

LP concentrated seawater discharge valve 8 is opened under the control force, and the concentrated seawater at the rod end of the seawater cylinder is discharged. At this time, the HP concentrated seawater inlet valve 7 is closed due to the HP concentrated seawater from the RO membrane module and the spring force. Next working state piston moves to the left, HP raw seawater discharge valve 10 is opened, HP raw seawater enters the RO membrane module. LP raw seawater inlet valve 9 is closed under the action of spring force and HP raw seawater, Therefore, the pressurized HP raw seawater will not flow back to the water tank. At the same time, the control force overcomes the spring force of the HP concentrated seawater inlet valve 7 to open the HP concentrated seawater inlet valve 7, HP concentrated seawater enters the rod side of seawater cylinder, its pressure acts on the annular area of the rod end, and together with the power F, pressurizes the raw seawater to achieve the required pressure.

2.2. Integrated system

In order to control the switch of HP concentrated seawater inlet valve 7 and LP concentrated seawater outlet valve 8, the movement speed of the piston and the force F acting on the piston rod, a special electro-hydraulic proportional system is proposed. This innovatively integrates the rigid piston of the hydraulic cylinder and the seawater cylinder and realizes the synchronous movement of the hydraulic cylinder and the seawater cylinder. A double hydraulic cylinder replaced traditional booster devices to generate pressure. The output pressure and displacement can be real-time feedback compensation. Sensors, amplifiers, and the pilot proportional direction valve constitute a closed-loop control, and its means of pressure and ERD are a whole. The hydraulic principle is shown in Fig. 2. The controller and circuit system are not shown in Fig. 2. The integrated system of electro-hydraulic proportional control pressurization and energy recovery proposed in this paper is suitable for water production of 0–1,500 m^3/d, which can be changed by changing the speed of the hydraulic cylinder.

The constant pressure variable displacement pump11 of Rexroth A4VSO125DR30RNBRPB is used as a power source and matches automatically according to the flow rate required by the system. The pilot operated proportional directional valve 4WRKE16E125P-3X with electrical position feedback and integrated electronic components (hereinafter referred to as proportional valve), which is used to control the pressure and flow of the hydraulic cylinder, because the seawater cylinder and the hydraulic cylinder are rigidly connected, thus controlling the pressure and speed of the seawater cylinder. The oil from constant pressure variable displacement pump 11 is divided into three parts, with part one into the proportional valve 22, part two into the proportional valve 38, the last part into the pressure reducing valve 15 as the control oil. Proportional valve 22 moves right under the control of the controller, controlling the piston of hydraulic cylinder 46 and marine cylinder 44 to move right. At the same time, the electromagnet 6DT of electromagnetic directional valve 25 gets electricity. Then the left side control pilot controlling check valve in the seawater hydraulic lock 27 that is connected with electromagnetic directional valve 25 is closed to controls the high-pressure concentrated seawater to enter the rod chamber of seawater cylinder through seawater hydraulic lock 27 without directly discharging through seawater hydraulic lock 27. The energy of high-pressure concentrated seawater and the hydraulic cylinder is used to pressurize raw seawater without the rod chamber into the RO membrane module. The controller controls the proportional valve 38 to move left, the piston of the hydraulic cylinder 43 and the seawater cylinder 41 to move right, and the electromagnet 8DT of the electromagnetic directional valve 35 to gets power. The left hydraulic controlling one-way valve in the seawater hydraulic lock 34 that is connected with the electromagnetic directional valve 35 is closed, which means that the channel through which the high-pressure concentrated seawater enters the rod cavity of the seawater cylinder 43 is closed, After discharging the concentrated seawater after work, the raw seawater enters the rodless chamber of seawater cylinder 41 through pilot operated check valve group 32. The displacement sensor monitors the displacement of the hydraulic cylinder in real-time, and the pressure sensor monitors the pressure of the hydraulic cylinder and the sea cylinder respectively. Under the control of the cooperative control strategy, the hydraulic cylinder 46 and the sea cylinder 45 runs to the endpoint according to the given target, that is, the left subsystem completes the recovery of pressure energy in the concentrated seawater while pressurizing the raw seawater, and the right

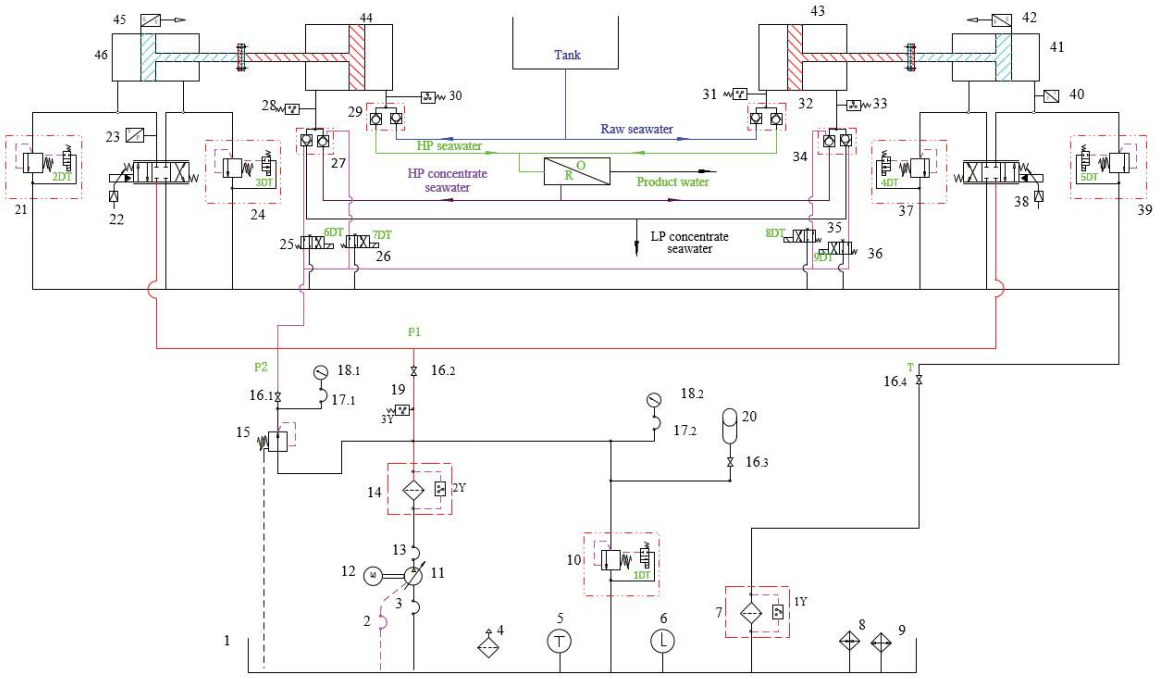

Fig. 2. Schematic diagram of the integrated system of electro-hydraulic proportional control pressurization and energy recovery. (1) Hydraulic tank; (2) oil drain pipe; (3) oil suction pipe; (4) air cleaner; (5) temperature sensor; (6) level sensor; (7) filter; (8) heater; (9) cooler; (10/21/24/37/39) solenoid pressure relief valves; (11) constant pressure variable displacement pump; (12) motor; (13/17) pipe; (14) HP filter; (15) pressure reducing valve; (16) cutoff valve; (18) pressure gauge; (19/28/30/31/33) pressure-relay; (20) spring-loaded hydraulic accumulator; (22/38) pilot operated proportional directional valve; (23/40) pressure sensor; (25/26/35/36) electromagnetic directional valve; (27/29/32/34) seawater hydraulic lock; (41/46) hydraulic cylinder; (43/44) seawater cylinder; (42/45) position sensor.

subsystem operates according to the given target. When the concentrated seawater is discharged and the raw seawater is inhaled, a movement is completed. In the next cycle, the left subsystem exchanges with the right subsystem, that is, the left subsystem discharges the working concentrated seawater and inhales the raw seawater at the same time; the right subsystem completes the recovery of the pressure energy in the concentrated seawater while pressurizing the raw seawater, in turn, to ensure that the raw seawater with stable pressure and the flow enters the RO membrane group. In the file, the workflow is shown in Fig. 3.

2.3. Mathematical model of the integrated system

2.3.1. Theoretical mathematical model

At present, the design of desalination pressurization and energy recovery system mainly depends on data and experience, and the theoretical and mathematical models of the desalination systems are relatively few. Starting from the mathematical model of the electro-hydraulic proportional valve-controlled cylinder, this paper regards the motion characteristics of the seawater cylinder and the flow characteristics of raw seawater and concentrated seawater as a load of the electro-hydraulic proportional valve-controlled cylinder. According to the seawater properties of the Bohai Bay of Pacific, as shown in Table 1, the Dow desalination membrane is selected and establishes the pressure and flow characteristics equation of the RO membrane module by studying the performance of the Dow membrane in the United States and relevant literature [10,22,30].

$$Q = A\left(\Delta P - \Delta\pi\right) \tag{1}$$

$$P = A_k Q + b \tag{2}$$

where Q is the permeate flow rate through the membrane, A is the membrane area, ΔP and $\Delta\pi$ are the applied hydraulic pressure differential and the OPD across the membrane, respectively. Eq. (2) represents the linear relationship between feed pressures and permeate flow rate, and coefficients derived from Eq. (1) for A_k and b.

In most hydraulic systems controlled by electro-hydraulic proportional valves, the dynamic response speed of general proportional valves is often much higher than that of hydraulic power components. In order to simplify the mathematical model of the system, the mathematical model of the proportional valve is equivalent to the second-order oscillation element. If the natural frequency of the proportional valve is higher than the natural frequency of the hydraulic power element, the transfer function of the proportional valve can also be represented by a first-order inertial element. When the natural frequency of the proportional valve is far greater than the natural frequency of the power element (usually more than 10 times), the proportional valve can be regarded as a proportional

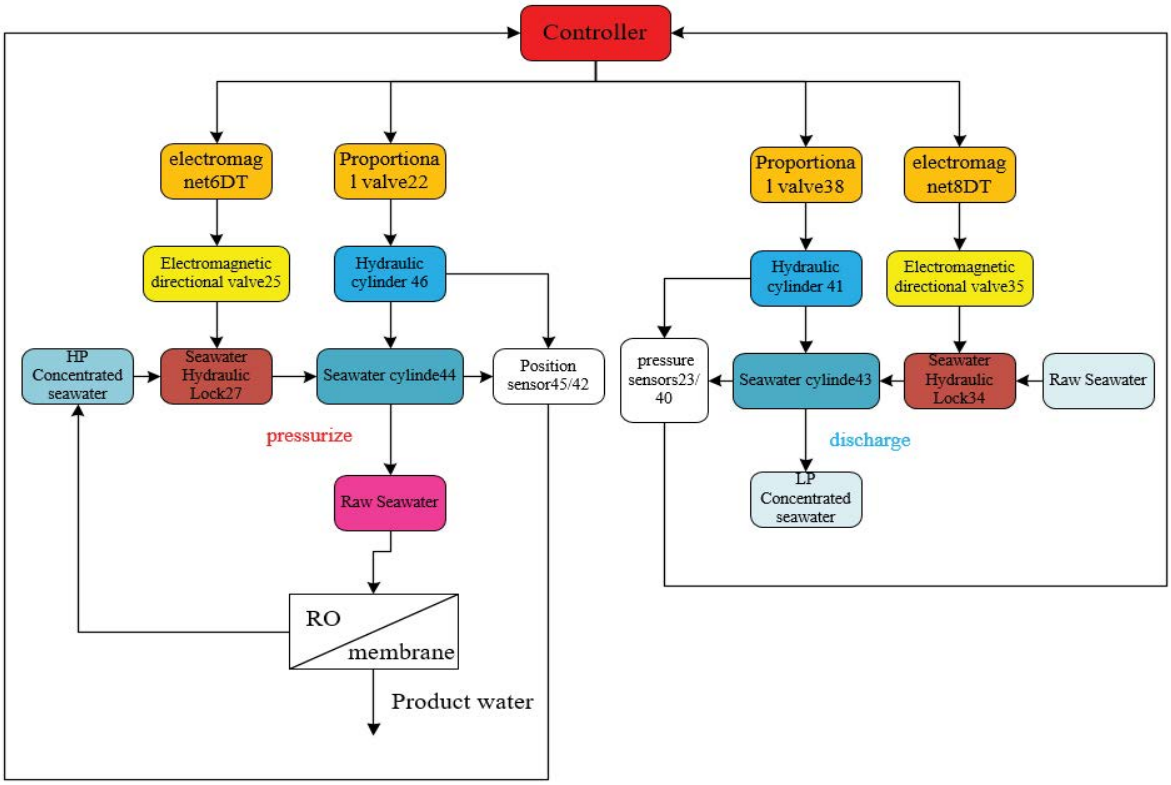

Fig. 3. Workflow diagrams.

Table 1
Composition of seawater from Bohai Bay of Pacific

Solute species	Concentration (mg/L)
Cl^-	17,500
Na^+	10,000
Mg^{+2}	1,150
Ca^{+2}	350
SO_4^{-2}	2,500
K^+	350
Total dissolved solids	32,000

element. In this system, the hydraulic natural frequency is about 9 Hz, and the natural frequency of the proportional reversing valve is 25 Hz. Therefore, the proportional reversing valve can be equivalent to the transfer function of the proportional reversing valve with inertia link as Eq. (3):

$$\frac{Q}{I} = \frac{K_q}{\frac{s}{\omega_v} + 1} \tag{3}$$

where K_q is the flow gain of the proportional valve, and ω_v is the phase width of the proportional valve.

The system uses the proportional directional valve to control the hydraulic cylinder to push the piston movement of the seawater cylinder, thus, the output pressure of the seawater cylinder can be controlled. The diagram of the control mechanism is shown in Fig. 4.

The following assumptions are used to establish the mathematical model of the system:

- The hydraulic pipeline connecting the hydraulic cylinder and the proportional valve is short and thick enough;
- Both internal and external leakage of the hydraulic cylinder is laminar flow.
- The pressure loss of the connecting pipeline can be neglected.
- In the hydraulic system, the supply pressure of the system is approximately constant, and the return pressure of the system is zero.
- When the hydraulic system works, the oil temperature and the elastic modulus of the oil in the system are approximately constant.

When the hydraulic cylinder pressurizes the seawater cylinder, the piston rod extends outward. At this time, the system is analyzed.

$$n = \frac{A_2}{A_1} \tag{4}$$

where n is the effective area ratio of the rod cavity with the rod cavity of the hydraulic cylinder.

Define the load pressure of the hydraulic cylinder as Eq. (5):

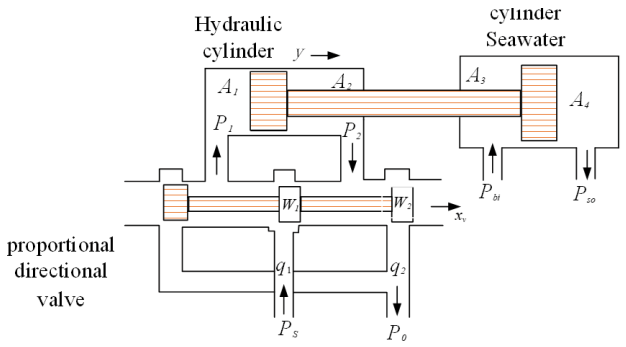

Fig. 4. Diagram of the control mechanism.

$$P_L = \frac{F}{A_1} = P_1 - \frac{A_2}{A_1}P_2 = P_1 - nP_2 \tag{5}$$

The load flow rate of the hydraulic cylinder is defined. When the piston rod extends outward, the flow equation of the hydraulic cylinder without the rod cavity is Eq. (6), and the flow equation of the hydraulic cylinder with a rod cavity is Eq. (7).

$$Q_1 = C_d W x_v \sqrt{\frac{2}{\rho}\left(P_S - P_1\right)} \tag{6}$$

$$Q_2 = C_d W x_v \sqrt{\frac{2}{\rho}P_2} \tag{7}$$

Here C_d is proportional to the flow coefficient of the reversing valve, ρ is the average density of the fluid.

When the piston rod of the hydraulic cylinder moves, the system remains stable and the flow continuity equation in hydrodynamics can be obtained:

$$\frac{Q_2}{Q_1} = \sqrt{\frac{P_2}{P_S - P_1}} = n \tag{8}$$

The output power equation of the hydraulic cylinder is as follows:

$$N = P_1Q_1 - P_2Q_2 = P_LQ_L \tag{9}$$

From Eqs. (4), (8) and (9), the output power and the flow rate of the hydraulic cylinder can be calculated as follows:

$$N = \left(P_1 - nP_2\right)Q_1 = P_LQ_1 \tag{10}$$

$$Q_L = Q_1 = \frac{Q_1 + nQ_2}{1+n^2} \tag{11}$$

where Q_L is the load flow rate of the hydraulic system.

When the piston rod of the hydraulic cylinder extends out, the flow rate into the rodless chamber of the hydraulic cylinder is as follows:

$$Q_1 = \frac{dV_1}{dt} + \frac{V_1}{\beta_e}\frac{dP_1}{dt} + C_{ip}\left(P_1 - P_2\right) + C_{ep}P_1 \tag{12}$$

The flow rate out of the rod cavity of the hydraulic cylinder is as follows:

$$Q_2 = C_{ip}\left(P_1 - P_2\right) - \frac{dV_2}{dt} - \frac{V_2}{\beta_e}\frac{dP_2}{dt} - C_{ep}P_2 \tag{13}$$

Here C_{ip} is the internal leakage system of the hydraulic cylinder; C_{ep} is the external leakage coefficient of the hydraulic cylinder; V_1 is the volume of the rodless chamber of the hydraulic cylinder (including oil intake chamber, connecting pipeline and valve) $V_1 = V_{10} + A_1x_p$; V_2 is the volume of rod cavity of the hydraulic cylinder (including oil intake chamber, connecting pipeline and valve) $V_2 = V_{20} - A_2x_p$; β_e is the effective bulk modulus of elasticity.

From the above equation, the load flow rate of the hydraulic cylinder can be calculated as follows:

$$Q_L = Q_1 = C_{ie}P_L + C_fP_s + \frac{V_t dP_L}{4\beta_e dt} + A_1\frac{dx_p}{dt} \tag{14}$$

where C_{ie} is the equivalent total leakage coefficient of hydraulic cylinder and can be calculated with the following formula:

$$C_{ie} = \frac{C_{ip}(1+n)}{n^3+1} + \frac{C_{ep}}{1+n^2}$$

C_f is the equivalent internal leakage coefficient of the hydraulic cylinder and can be calculated with the following formula:

$$C_f = \frac{n^2\left(n^2-1\right)C_{ip}}{\left(n^3+1\right)\left(1+n^2\right)}$$

V_t is the equivalent volume and can be calculated with the following formula:

$$V_t = \frac{4V_1}{n^2+1}$$

The following equation can be obtained by linearizing the flow equation of the proportional valve.

$$Q_L = K_qx_v - K_cP_L \tag{15}$$

Usually, in the hydraulic system, the load force of the system mainly includes viscous resistance, elastic force, inertia force, and external load force. From the balance of output force and load force of the hydraulic cylinder, the following equation can be obtained.

$$A_1P_1 - A_2P_2 + A_3P_{bi} - A_2P_{so} = m_t\frac{d^2x_p}{dt^2} + B_p\frac{dx_p}{dt} + Kx_p \tag{16}$$

where P_{bi} is the pressure of HP concentrate seawater and P_{so} is the pressure of the pressurized raw seawater.

In order to ensure that the raw seawater entering the RO membrane module has a stable flow rate, the sum of the pressurized raw seawater flow of two seawater cylinders is a constant, which can be indicated by the following publication.

$$A_4 \frac{dx_{p1}}{dt} + A_4 \frac{x_{p2}}{dt} = Q \tag{17}$$

The following equations can be obtained by Laplace transformation of Eqs. (14)–(17):

$$Q_L = K_q x_v - K_c P_L \tag{18}$$

$$Q_L = A_1 s x_p + \frac{V_t}{4\beta_e} s P_L + C_{ie} P_L + C_f P_s \tag{19}$$

$$A_1 P_1 - A_2 P_2 + A_3 P_{bi} - A_4 P_{so} = \left(m_t s^2 + B_p s + K\right) x_p \tag{20}$$

$$A_4 x_{p1} s + A_4 x_{p2} s = Q_{so} \tag{21}$$

In the electro-hydraulic proportional control based pressurization and integration system, two hydraulic cylinders and two seawater cylinders are used to realize the pressurization and energy recovery of raw seawater. Using the above equations the block diagram of the transfer function of the system is established, as shown in Fig. 5. Among them, u_1 and u_2 represent the given signals of two hydraulic cylinders, K_1 represents the coefficient of the proportional amplifier, $K_{sv}G_{sv}$ represents the transfer function of the proportional valve, and K_f is the transfer function of displacement sensor, that is, the proportional link is constant.

2.3.2. MATLAB/Simulink simulation method

At present, Simulink software has been widely used and recognized in the field of electro-hydraulic system simulation and has gradually become a powerful tool to solve practical problems of the hydraulic system. According to the mathematical model, the simulation model of electro-hydraulic proportional control based pressurization and energy recovery integrated system is established in Simulink software.

3. Results and discussion

If a system wants to work normally, it must ensure its stability. Generally speaking, the amplitude-frequency and phase-frequency characteristics of the control system can reflect the stability of the system well, and the dynamic characteristics of the system can be seen through software analysis. In the Simulink software, the stability of the system is analyzed. The logarithmic Bode diagram of the system can be obtained by linear analysis options. As shown in Fig. 6, the gain margin is 8.48, while the phase margin is 171. The system is stable.

The coordinated control strategy of two cylinders is adopted to ensure a smooth transition when two cylinders are switched. The input signals of two cylinders are Eqs. (22) and (23). In continuous operation, the controller is used to cycle.

$$u_1 = \begin{cases} 0.1 \times t & 0 < t \le 9 \\ -0.05 \times t^2 + t - 4.05 & 9 < t \le 10 \\ 0 & 10 < t \le 19 \\ 0.05 \times t^2 - 1.9 \times t + 18.05 & 19 < t \le 20 \end{cases} \tag{22}$$

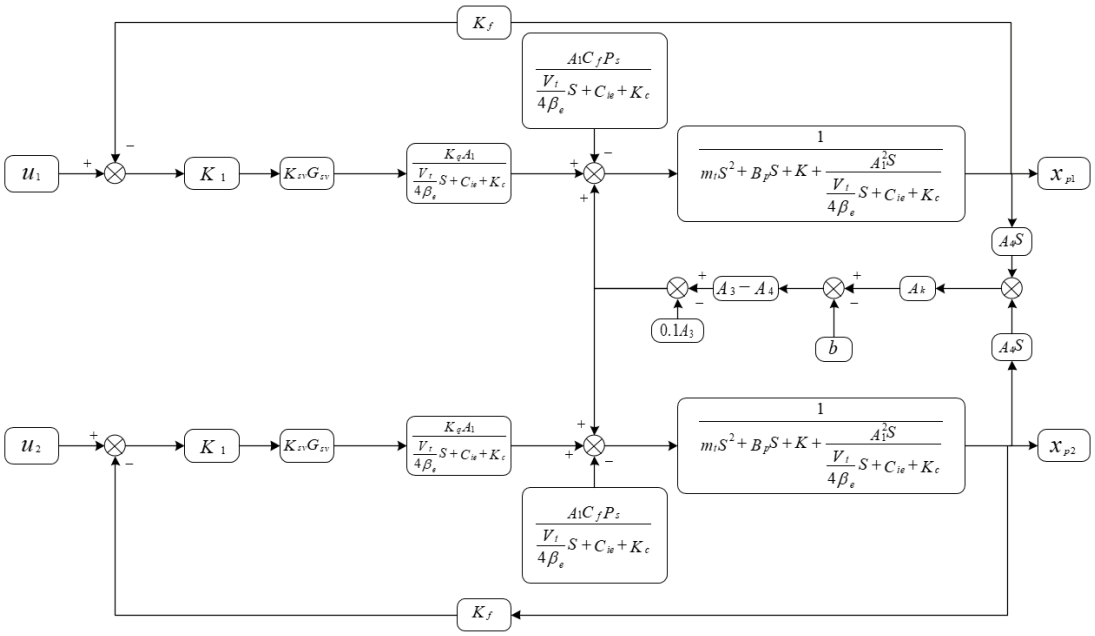

Fig. 5. Block diagram of the transfer function.

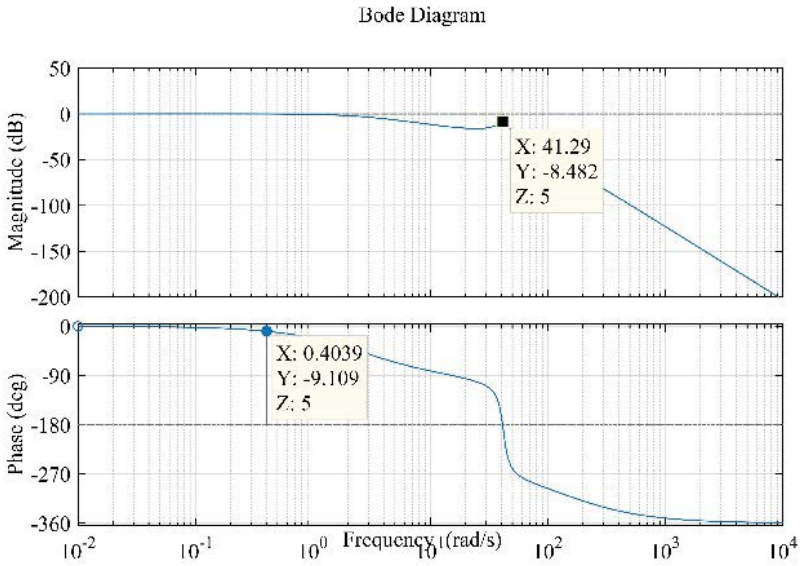

Fig. 6. System Bode diagram.

$$u_2 = \begin{cases} 0 & 0 < t \le 9 \\ 0.05 \times t^2 - 0.9 \times t + 4.05 & 9 < t \le 10 \\ 0.1 \times t - 0.95 & 10 < t \le 19 \\ -0.05 \times t^2 + 2 \times t + 19 & 19 < t \le 20 \end{cases} \quad (23)$$

Fig. 7 shows the seawater pressure curve of the high-pressure raw material in the RO membrane module after pressurization by the electro-hydraulic-proportion-control-based pressure and energy recovery integrated system obtained via Simulink software. Within 0–2 s, the pressure rises from 0 to 7 MPa, and the system reacts quickly and smoothly. When the two cylinders are switched, the pressure fluctuation occurs at around 10th second, with the pressure being 6.5 MPa, the lowest point. The range of pressure fluctuation is small. According to the relevant literature and the Dow's Membrane Performance Manual of the United States, this paper chooses the linear relationship between pressure and flow.

Fig. 8 shows the flow curve of high-pressure raw water entering the RO membrane module. The trend of change is consistent with the pressure curve. Its flow rate is 157 L/min and also fluctuates at about 10th second. The lowest point is 146 L/min. The flow rate quickly becomes stable. This paper only simulates the start-up moment and a commutation period, after which the curve will reproduce the waveform from 10th to 20th seconds continuously.

The design scheme and control strategy are used to verify the experiment. The experimental equipment is shown in Fig. 9. Because of the corrosiveness of seawater, there is no flow rate sensor installed at the outlet of the seawater cylinder. The flow rate of raw material seawater is obtained indirectly through the flow rate of the hydraulic cylinder, because the piston of the hydraulic cylinder and seawater cylinder is rigidly connected and has the same speed, so the flow rate of both is proportional, as shown in Eq. (24). Therefore, the correctness and accuracy of the simulation

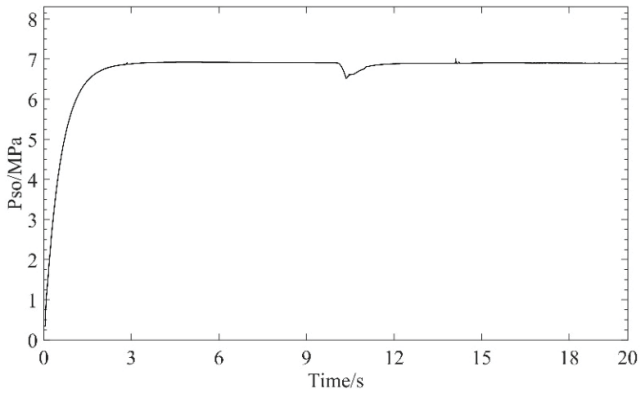

Fig. 7. Pressure curve of raw material seawater.

can be verified by comparing the simulation and experimental curves of the flow rate of the hydraulic cylinder, and the pressure and flow rate of the raw material seawater can be obtained.

$$\frac{A_1}{A_4} = \frac{A_1^v}{A_4^v} = \frac{Q_h}{Q_{so}} = n_{hr} \quad (24)$$

where A_1 is the effective area of the rodless chamber of hydraulic cylinder, A_4 is the effective area of seawater cylinder without rod cavity, v is the speed of the hydraulic cylinder, Q_h is the flow rate of the rodless chamber of the hydraulic cylinder during pressurization, n_{hr} is the area ratio coefficient.

The flow rate simulation curve of the hydraulic cylinder is obtained by multiplying the raw material seawater flow by the area ratio coefficient n_{hr}, as shown in Fig. 10. The black curve is the flow rate simulation curve of the hydraulic cylinder, and the red curve is the experimental test curve. The simulation and the experimental curve are in good

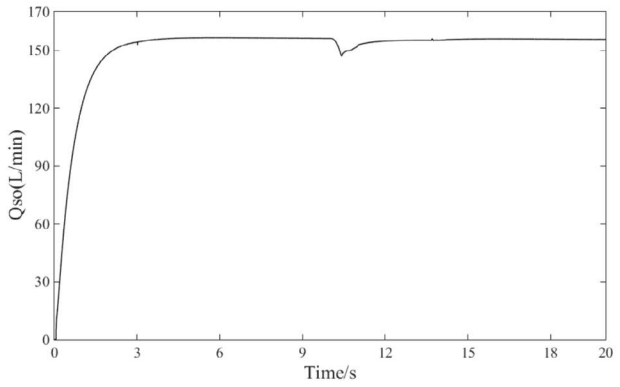

Fig. 8. Feed flow curve of raw seawater after pressurization.

agreement with each other, and the changing trend is the same. However, due to the simplification of some nonlinear conditions, there is a small steady-state error of about 0.8 L/min in the simulation and experiment, which can verify the accuracy of the mathematical model and simulation results. So Figs. 7 and 8 can be used as the pressure and flow rate curves of the actual raw material seawater. According to the performance parameters of the RO membrane, it can be known that the product water flow rate is 40% of the raw material seawater flow rate.

In order to obtain the SEC of the integrated system of electro-hydraulic proportional pressurization and energy recovery, in addition to the product water flow rate, the total energy consumption of the system is also needed. In this integrated system, the power required by a constant pressure variable pump is the power consumed by the total system, which is calculated by the following equation:

$$E_I = \frac{P_S Q_{IL}}{\eta} \tag{25}$$

where E_I is the power consumption of the system, P_S is the oil supply pressure of constant pressure variable displacement pump, Q_{IL} is the output flow rate of constant pressure variable displacement pump, η is the efficiency of constant pressure variable displacement pump, which is about 97%. In this system, the water recovery rate is 40%, and the SEC is calculated by Eq. (26).

$$\mathrm{SEC}_{net} = \frac{E_I}{Q_{so} \times 40\%} \tag{26}$$

The outlet pressure curve of the constant pressure variable displacement pump is the working pressure of the whole integrated system, as is shown in Fig. 11. Almost instantaneously achieve set pressures and maintain stability. Fig. 12 shows the outlet flow rate of the constant pressure variable displacement pump, which is required by the integrated system. In the range of 0–10 s, the trend of flow rate curve is consistent with the feed flow curve of raw seawater after pressurization. But in 10–20 s, one hydraulic cylinder extends to pressurize raw seawater while

Fig. 9. Experimental equipment.

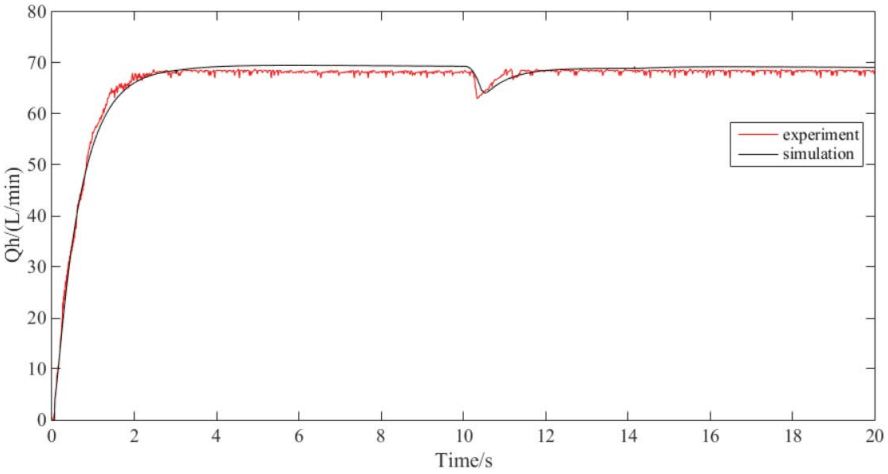

Fig. 10. Hydraulic cylinder simulation flow rate curve and experimental flow rate curve.

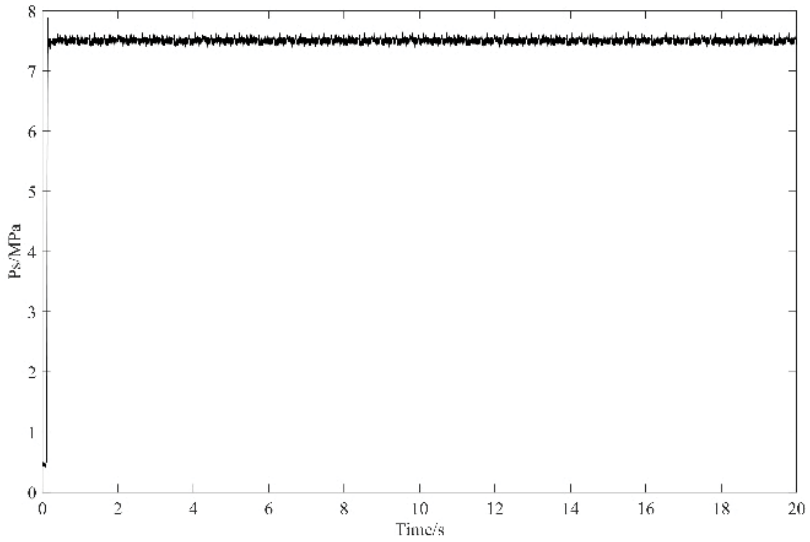

Fig. 11. Oil supply pressure curve of constant pressure variable displacement pump.

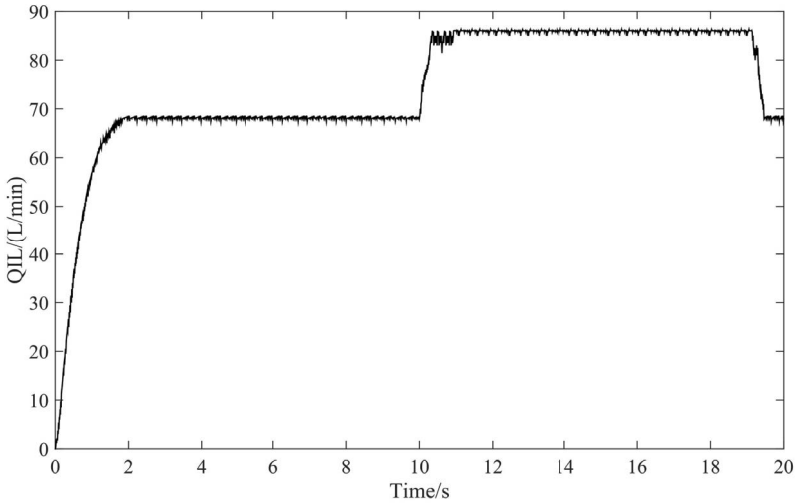

Fig. 12. The output flow rate of an integrated system.

the other retracts to suck in raw seawater. The flow rate required by the system is higher than before.

According to the measured curve, the SEC is 2.76 kWh/m^3, which is lower than the conventional desalination system [10,23].

4. Conclusion

In this paper, the energy consumption and ERD of the seawater desalination system are studied in depth. An integrated device of electro-hydraulic proportional control based pressurization and energy recovery is proposed. The device can recover the pressure energy of high-pressure concentrated seawater while pressurizing raw seawater. The device can adapt to different water recovery requirements by changing the diameter of the piston rod of the seawater cylinder. The mathematical model of the system is established theoretically. In order to reduce the pressure and flow fluctuation, a curve transition control strategy is adopted to realize the coordinated motion of the two cylinders. The stability and performance of the system are analyzed by simulation. The stability and rapidity of the electro-hydraulic proportional control based pressurization and energy recovery integrated device is good, which can satisfy the demand of seawater desalination.

Using theory and simulation technology to guide the installation and debugging of the experimental equipment, the output flow and pressure curves of constant pressure variable displacement pumps are measured. The average input power of the system is 10 kW and the SEC of the system is 2.76 kWh/m^3 when the water recovery rate is 40%, compared with the conventional desalination system, the energy consumption of the ERD and system proposed in this paper is reduced by 18%. Thanks to the high power density of the hydraulic system, the whole desalination system has a compact structure and can be simple.

Acknowledgment

This research grant was supported by the Qinhuangdao Yongchunjie seawater desalination technology engineering Co., Ltd.

References

[1] Y.H. Teow, A.W. Mohammad, New generation nanomaterials for water desalination: a review, Desalination, 451 (2019) 2–17.
[2] W.L. Ang, A.W. Mohammad, N. Hilal, C.P. Leo, A review on the applicability of integrated/hybrid membrane processes in water treatment and desalination plants, Desalination, 363 (2015) 2–8.
[3] T. Distefano, S. Kelly, Are we in deep water? Water scarcity and its limits to economic growth, Ecol. Econ., 146 (2018) 130–147.
[4] M. Elimelech, W.A. Phillip, The future of seawater desalination: energy, technology, and the environment, Science, 333 (2011) 712–717.
[5] P.S. Goh, T. Matsuura, A.F. Ismail, N. Hilal, Recent trends in membranes and membrane processes for desalination, Desalination, 391 (2016) 43–60.
[6] M.N.A. Hawlader, J.C. Ho, C.K. Teng, Desalination of seawater: an experiment with RO membranes, Desalination, 132 (2000) 275–280.
[7] Y.M. Kim, S.J. Kim, Y.S. Kim, S. Lee, I.S. Kim, J.H. Kim, Overview of systems engineering approaches for a large-scale seawater desalination plant with a reverse osmosis network, Desalination, 238 (2009) 312–332.
[8] M.A. Jamil, B.A. Qureshi, S.M. Zubair, Exergo-economic analysis of a seawater reverse osmosis desalination plant with various retrofit options, Desalination, 401 (2017) 88–98.
[9] J. Imbrogno, J.J. Keating IV, J. Kilduff, Critical aspects of RO desalination: a combination strategy, Desalination, 401 (2017) 68–87.
[10] M. Göktuğ Ahunbay, Achieving high water recovery at low pressure in reverse osmosis processes for seawater desalination, Desalination, 465 (2019) 58–68.
[11] H. Sakai, T. Ueyama, M. Irie, K. Matsuyama, A. Tanioka, K. Saito, A. Kumano, Energy recovery by PRO in sea water desalination plant, Desalination, 389 (2016) 52–57.
[12] A. Subramani, M. Badruzzaman, J. Oppenheimer, J.G. Jacangelo, Energy minimization strategies and renewable energy utilization for desalination: a review, Water Res., 45 (2011) 1907–1920.
[13] Y. Wang, S.C. Wang, S.C. Xu. Experimental studies on dynamic process of energy recovery device for RO desalination plants, Desalination, 160 (2004) 187–193.
[14] D.W. Song, Y. Wang, S.C. Xu, J.P. Gao, Y.F. Ren, S.C. Wang, Analysis, experiment and application of a power-saving actuator applied in the piston type energy recovery device, Desalination, 361 (2015) 65–71.
[15] D.W. Song, Y. Wang, S.C. Xu, Z.C. Wang, H. Liu, S.C. Wang, Control logic and strategy for emergency condition of piston type energy recovery device, Desalination, 348 (2014) 1–7.
[16] J. Zhou, Y. Wang, Z.M. Feng, Z.S. He, S.C. Xu, Effective modifications of reciprocating-switcher energy recovery device by adopting pilot valve plates to decrease the switching load and fluid fluctuations, Desalination, 462 (2019) 39–47.
[17] N. Liu, Z.L. Liu, Y.X. Li, L.X. Sang, Studies on leakage characteristics and efficiency of a fully-rotary valve energy recovery device by CFD simulation, Desalination, 415 (2017) 40–48.
[18] N. Liu, Z.L. Liu, Y.X. Li, L.X. Sang, An optimization study on the seal structure of fully-rotary valve energy recovery device by CFD, Desalination, 459 (2019) 46–58.
[19] B. Peñate, L. García-Rodríguez, Energy optimisation of existing SWRO (seawater reverse osmosis) plants with ERT (energy recovery turbines): technical and thermoeconomic assessment, Energy, 36 (2011) 613–626.
[20] S. Bross, W. Kochanowski, SWRO core hydraulic system: extension of the SalTec DT to higher flows and lower energy consumption, Desalination, 203 (2007) 160–167.
[21] S. Schafer, New Pressure Exchanger Design Concept for Sustainable, Long Term Costing Saving, IDA World Congress, 2011.
[22] Y. Wang, Y.F. Ren, J. Zhou, E.L. Xu, S.C. Xu, Functionality test of an innovative single-cylinder energy recovery device for SWRO desalination system, Desalination, 388 (2016) 22–28.
[23] J.X. Sun, Y. Wang, S.C. Xu, Y.X. Wang, Performance prediction of hydraulic energy recovery (HER) device with novel mechanics for small-scale SWRO desalination system, Desalination, 249 (2009) 667–671.
[24] A. Efraty, Closed circuit desalination series no-6: conventional RO compared with the conceptually different new closed circuit desalination technology, Desal. Water Treat., 41 (2012) 279–295.
[25] M.A. Sanza, V. Bonnélyea, G. Cremerb, Fujairah reverse osmosis plant: 2 years of operation, Desalination, 203 (2007) 91–99.
[26] T.H. Chong, S.-L. Loo, W.B. Krantz, Energy-efficient reverse osmosis desalination process, J. Membr. Sci., 473 (2015) 177–188.
[27] J.B. Kim, S.K. Hong, A novel single-pass reverse osmosis configuration for high-purity water production and low energy consumption in seawater desalination, Desalination, 429 (2018) 142–154.
[28] T.H. Chong, S.-L. Loo, A G. Fane, W.B. Krantz, Energy-efficient reverse osmosis desalination: effect of retentate recycle and pump and energy recovery device efficiencies, Desalination, 366 (2015) 15–31.
[29] K.H. Jeong, M.K. Park, T.H. Chong, Numerical model-based analysis of energy-efficient reverse osmosis (EERO) process: performance simulation and optimization, Desalination, 453 (2019) 10–21.
[30] H.-J. Oh, T.-M. Hwang, S. Lee, A simplified simulation model of RO systems for seawater desalination, Desalination, 238 (2009) 128–139.

Appendix: parameter table

Structural parameters of electro-hydraulic proportional control pressurization and energy recovery integrated system

Parameter	Value	Unit
Throttle coefficient, C_d	0.65	
Effective area of rodless chamber of hydraulic cylinder, A_1	0.0113	m^2
Effective area of rod cavity of hydraulic cylinder, A_2	0.001695	m^2
Area ratio of hydraulic cylinder, n	0.15	
Effective area of rod cavity in seawater cylinder, A_3	0.01527	m^2
Effective area of seawater cylinder without rod cavity, A_4	0.02545	m^2
Area ratio of seawater cylinder, n_h	0.6	
Equivalent mass, m_t	1.2×10^4	Kg
Elastic modulus of hydraulic oil, β_e	700×10^6	Pa
Modulus of elasticity of seawater, β_{es}	2.34×10^9	Pa
Viscous damping coefficient, B_p	800	N(m/s)
Leakage coefficient in hydraulic cylinder, C_{ic}	3×10^{-11}	m^3/(s Pa)
Hydraulic cylinder outside leakage coefficient, C_{ec}	0	m^3/(s Pa)